

LOAD REDISTRIBUTION AT THE FIRST STORY OF A MID-RISE RC FRAME BUILDING

Hakim BECHTOULA^{*1}, Susumu KONO^{*2} and Fumio WATANABE^{*3}

ABSTRACT

Experimental and analytical results of two 1/2-scale RC model frames with two stories and one span are reported in this paper. The frames were subjected to vertical and cyclic lateral loads to investigate the force redistribution at the lower part of an eleven-story RC frame building. It was found that axial compression force representing 33% of the frame horizontal load carrying capacity was generated in the first floor beam. This axial force had an impact on the beam-column joint flexural strength ratio. Shift of the contraflexure point of the first story columns influenced considerably the curvature distribution of beam.

Keywords: reinforced concrete, frame, joint, elongation, contraflexure point, curvature

1. INTRODUCTION

Numerous researchers have performed cyclic tests on isolated reinforced concrete columns [1]. However, far fewer tests have been performed on statically indeterminate, multi-story, reinforced concrete frames [2]. Such tests are needed to experimentally evaluate the complex interaction among columns, beams and joints during cyclic loading. Especially the shear force at the column bases which is expected to be different from one column to another due to two major reasons. The first reason is that the flexural stiffness changes depending on the axial force intensity [3]. The second reason is that length of beam and columns changes with relatively large amount as reported by Stanton et al. [4]. It was also reported [5] that the change of member length caused erroneous prediction in force distribution at member. Among the objectives of this research is to: 1) Assess the effect of the shift of the contraflexure point of the first story columns, 2) evaluate the intensity of the generated axial load in beam and its effect on the beam-column joint's flexural strength ratio.

2. TEST PROGRAM

Two 1/2-scale RC frame representing the lower two stories of an eleven RC frame building

were tested under variable axial load and cyclic horizontal loads. Axial load, N , was varied linearly to the shear force, H , as: $N = 3000 \pm 5H(kN)$. The specimen's configuration as well as the test setup can be seen in **Fig. 1**. The cross section of the column was 500 mm by 500 mm and 300 mm by 500 mm for beams. The height of the first story was 2000 mm and the beam span length was 3000 mm.

Both frames were identical in all aspect except in the column shear reinforcements ratio. These ratios were 1% and 0.5% for LN60 and QN60, respectively. **Table 1** summarizes the material characteristics and the test variable of the test.

Both frames were loaded with two cycles to the following drift percentage: ± 0.10 , ± 0.20 , ± 0.40 , ± 0.70 , ± 1.00 , ± 2.00 , ± 3.00 and ± 4.00 . More details about the test setup and the homemade load cell used at mid-span of beams shown in **Fig. 1** can be found elsewhere [6].

Table 1: Material and test variables

Frame designation	Material			Axial load N/fcD ²	Test variable -Column shear rebar-
	Concrete strength	Longitudinal rebar	Shear rebar		
LN60	36.0 MPa Ec=28GPa	Column 12D25 (2.43%) Fy=323 MPa	Beam 2D10@100 (0.47%) Fy=378 MPa	Max. Comp. 0.6 Min. Comp. 0.05	4D13@100 (1.0%) Fy=377 MPa Fu=579 MPa Es=173 Gpa
QN60		Beam 8D22 (2.06%) Fy = 378 MPa	Beam Fu=524 MPa Es=187GPa		2D13@100 (0.5%)

*1 Research Fellow, Dept. of Architecture and Architectural Eng., Kyoto University, JCI Member

*2 Associate Professor, Dept. of Architecture and Architectural Eng., Kyoto University, JCI Member

*3 Professor, Dept. of Architecture and Architectural Eng., Kyoto University, JCI Member

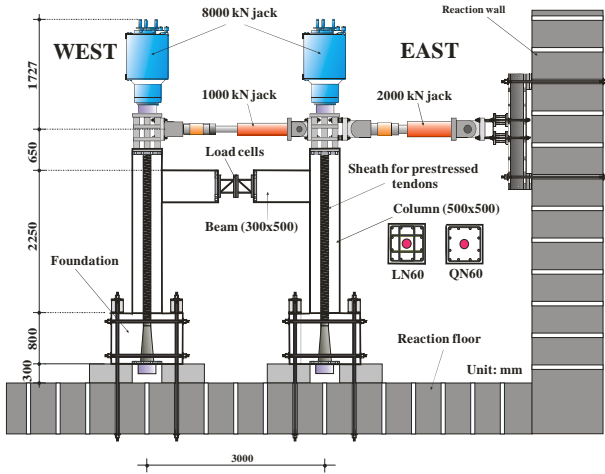


Fig. 1: Frame configuration and test setup

3. TEST RESULTS

3.1 Load-drift relationships

An example of the load-drift relationship is shown in **Fig. 2** for LN60. The frame showed a stable hysteresis loops until 4% drift.

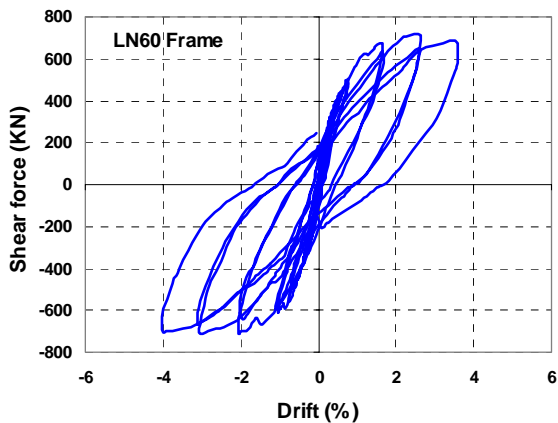


Fig. 2: Load-drift relation for LN60

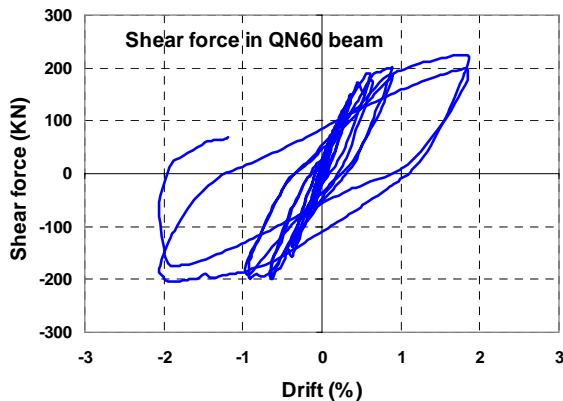
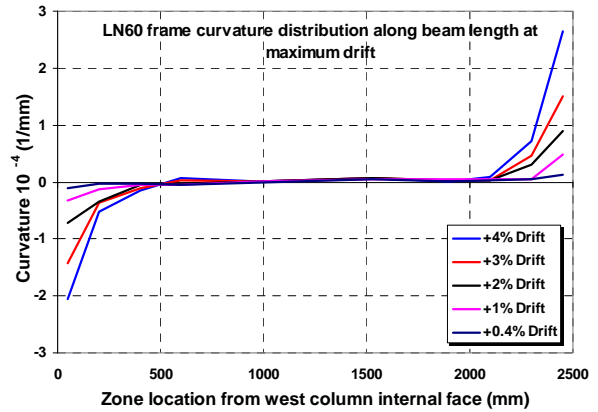


Fig. 3: Variation of the shear force in beam

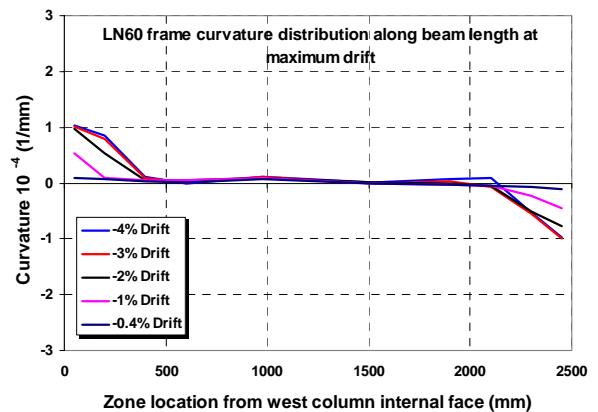
Axial, shear and bending moment at members were assessed using the load cell inserted at mid-span of the beam. **Fig. 3** shows the beam shear force versus the frame drift for QN60, as an example.

3.2 Shift of the contraflexure point

Using the displacement gauges attached along the beam length, curvature distribution was assessed for both frames. As an example, **Fig. 4** shows the curvature distribution for LN60 at each cycle along the beam length. It can be observed that beyond 2% of the positive drifts, curvatures at the beam-ends were nearly two times higher than those assessed during the negative drifts. This increase in the curvature distribution was due to the shift of contraflexure point at the first story columns as illustrated in **Fig. 5(a)** and discussed hereafter.



(a) Positive cycles



(b) Negative cycles

Fig. 4: Curvature distribution along the beam length of LN60

It is well known that curvature distribution, $\phi(x)$, and bending moment distribution, $M(x)$, at any section of the frame-member are related to

each other by:

$$EI\phi(x) = M(x) \quad (1)$$

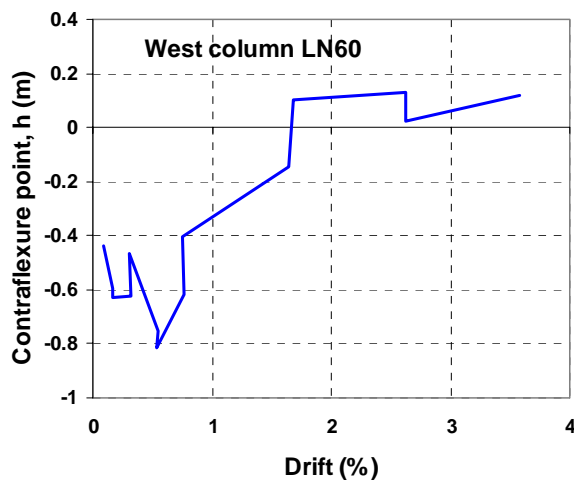
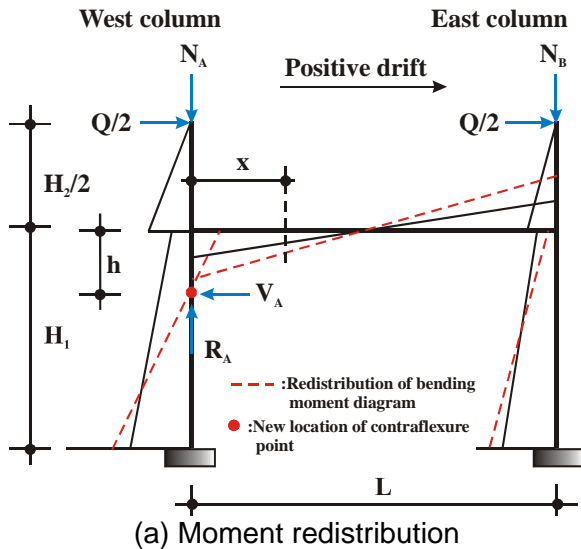
where E and I are the Young's modulus and moment of inertia, respectively.

Moment at a section distant from the left side of the beam by a distance of " x ", as shown in **Fig. 5(a)**, can be written as:

$$M(x) = V_A h + QH_2 / 4 - N_A x + R_A x \quad (2)$$

However, near the left side edge of the beam, the third and fourth terms of the right side of Eq. 2 can be neglected since the value of " x " is very small, hence, Eq. 2 can be rewritten as:

$$M(x) = V_A h + QH_2 / 4 \quad (3)$$



(b) Variation of the contraflexure point

Fig. 5: Variation of the moment redistribution due to the shift of the contraflexure point

In Eq. (2) and Eq. (3) the H_2 value corresponds to the height of the second story.

The increase of curvature at beam is due to the increase of bending moment given in Eq. 3, as a consequence of the increase in the lever arm of the shear force at column, h . Shift of the contraflexure points at columns were evaluated using the experimental recorded bending moment at beam edge, the applied horizontal load and the column shear force. **Fig. 5(b)** shows the variation of the contraflexure point at the west column of LN60. It was found that only in the west column under the positive cyclic loading that the contraflexure point, h , shifted from negative value to positive value, showing that the contraflexure point was shifted into the column as illustrated in **Fig. 5(a)**, which explain the difference in values of the curvature distribution shown in **Fig. 4**. The contraflexure point varied from -0.8 m to $+0.2$ m, which means that the lever arm of the column shear force, V_A , varied around 1 m. Shift of the lever arm toward column base, is due mainly to the degradation and damage of the column at the plastic hinge regions.

Effect of the lever arm variation on the seismic performance of the plastic hinge region cannot be captured by a cantilever column test, since the point of the application of the horizontal load is kept constant along the test. To take this effect into account, it is suggested that double flexure column test should be carried out instead of a single curvature column test, cantilever column.

4. ANALYSIS RESULTS

4.1 Prediction of Load-drift Relationships

The envelope curve of the load-drift relationship was calculated using the pushover analysis option in the nonlinear SAP2000 program [7]. Columns and beams were modeled with elastic beam elements as shown in **Fig. 6**, with plastic hinges at the ends having the characteristics, trilinear model, recommended by the Japanese design guidelines [8]. The model considers only the flexural deformations of the members. The pushover analysis was carried step by step, by incrementing the horizontal displacement until a collapse mechanism is reached.

Table 2: test and analysis results

Frame	Exp. (kN)		Analy. -SAP-(kN)		Analy./Exp.	
	Pos.	Neg.	Pos.	Neg.	Pos.	Neg.
LN60	709	-709	717	-717	1.01	1.01
QN60	709	-663	709	-709	1.00	1.07

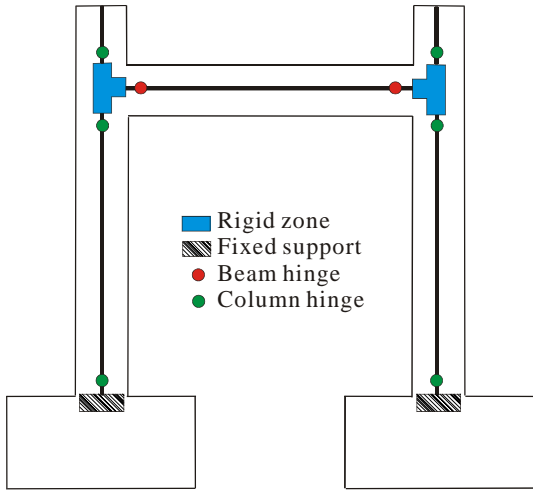
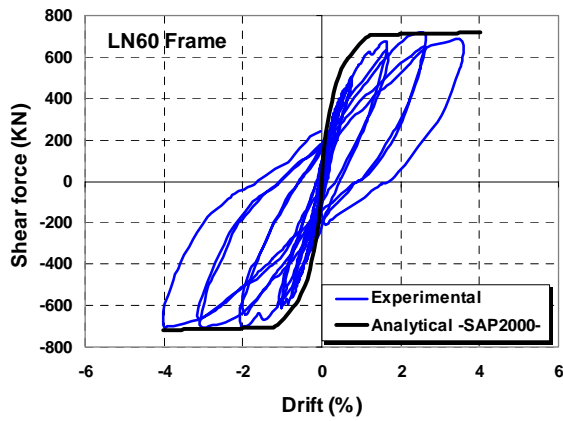
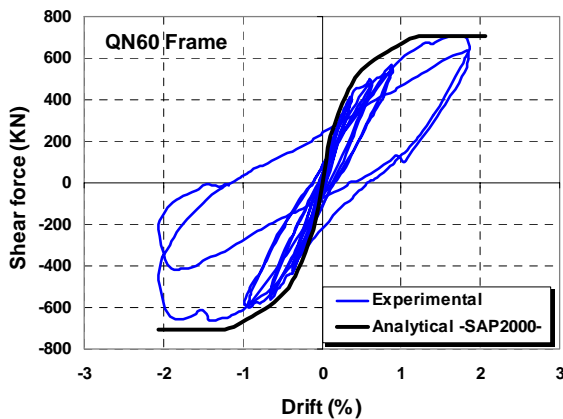


Fig. 6: Model for the frames



(a) LN60 frame



(b) QN60 frame

Fig. 7: Experimental and analytical frame load-drift relation

Beams and columns were modeled using the beam-element and at the beam-column joint panel rigid zones were inserted. A comparison between the experimental and analytical peak loads is given in **Table 2**. The experimental cyclic loading loops

and the analytical envelope curves are shown in **Fig. 7** for the two frames. It is clear from the figure that the analytical envelope curves fit quite well with the experimental hysteresis curves.

Good predictions were also found for the axial, shear and bending moment generated in the elements, beam and columns. As an example **Fig. 8** shows the prediction of the shear force at mid-span of QN60's beam and the shear force given by the load cell set at mid-span.

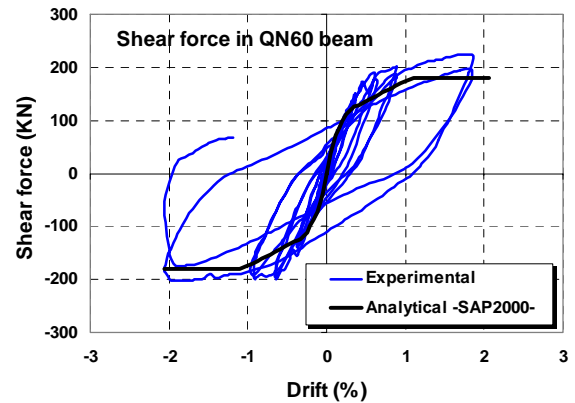


Fig. 8: Experimental and analytical beam shear force-drift relation

4.2 Prediction of the Axial load in Beam

In design practice, beams in a RC moment resisting frame building are designed under shear and bending moment only. However, axial load exists in reality due to the elongation of plastic hinge regions. Hereafter, a simple method for computing the probable axial compression force that may be developed in beams is proposed.

Using **Fig. 9(a)**, the shear force V_1 at column 1 can be determined using the beam shear force, V_b , and the beam axial load, N_b , as follows:

$$V_1 = \frac{1}{\alpha_1 h_1 + \alpha_2 h_2} (\alpha_2 h_2 N_b - M_b) \quad (4)$$

where, h_1 and h_2 are the height of the first story and second story, respectively. $\alpha_1 h_1$ and $\alpha_2 h_2$ are the distances from the center of the considered beam-column joint to the column's contraflexure points that can be determined by any kind of software. M_b is the beam moment at beam-column joint defined as $M_b = V_b L$, where L is half of the beam span length. Moment at the top of column 1 is found to be equal to:

$$M_1 = V_1 \alpha_1 h_1 = \frac{\alpha_1 h_1}{\alpha_1 h_1 + \alpha_2 h_2} (\alpha_2 h_2 N_b - M_b) \quad (5)$$

Solving Eq. 5 for N_b , Eq. 6 is obtained:

$$N_b = \frac{1}{\alpha_2 h_2} \left(\frac{\alpha_1 h_1 + \alpha_2 h_2}{\alpha_1 h_1} M_1 + M_b \right) \quad (6)$$

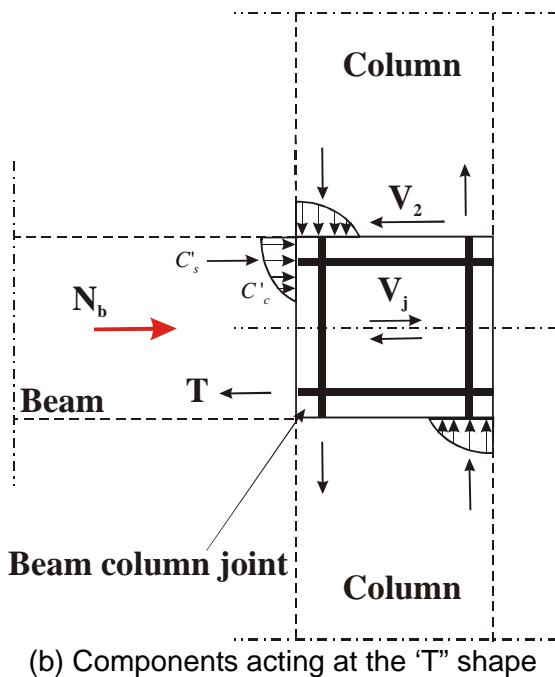
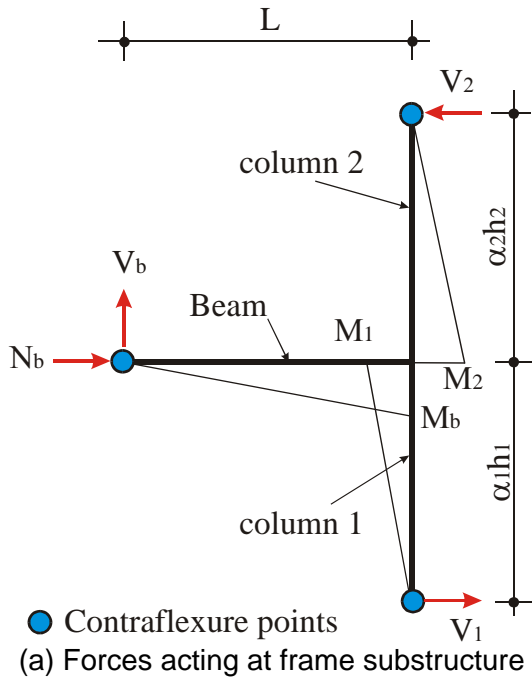


Fig. 9: Forces acting at different elements and joint of a RC "T" shape junction

Using Eq. 6 for the case of LN60 and taking M_b as the maximum flexural strength evaluated using the ACI code [10], the beam axial load was found to be $N_b = 238 \text{ kN}$. The values of α_i and M_i can be evaluated using the moment distribution of the frame computed by any kind of frame analysis program. In our case, α_2 was taken equal to 0.6 and the top moment of the first story M_1 was taken equal to zero, as found using the nonlinear SAP2000. The maximum axial load recorded by the load cell, N_{lc} , at mid-span of the beam during the test was $N_{lc} = 237 \text{ kN}$, which is exactly as the value computed using Eq. 6. The axial compression force in beam was 33% of the frame horizontal load carrying capacity. Presence of axial load in beams may lead to joint failure since, generally, during design phase beam are designed only for shear and bending. Damage can be important for "T" shape and "L" shape beam-column joints. In the contrary, for the cross shape "+", the presence of compressive force will act as a confinement for the beam column joint.

The forces acting at a "T" shape beam-column joint can be illustrated as shown in **Fig. 9(b)**. The definition of joint shear, V_j , as given in Eq. 7 was introduced by Hanson et al. [9], and is widely accepted and used nowadays. The joint shear means an internal force acting on the free body cut at the horizontal line at the mid height of the joint core as illustrated in **Fig. 9(b)**.

$$V_j = C'_s + C'_c - V_2 = T - V_2 \quad (7)$$

In Eq. 7, C'_c is the concrete compressive force, C'_s is the compressive force carried by the top reinforcement and T is the tensile force carried by the lower reinforcement. Eq. 7 was derived without axial force acting in beam. However, tested frame showed clearly the presence of axial load in beams, N_b . We suggest that Eq. 7 should be modified in order to take into account the real applied forces near the beam-column joint connection. Hence, Eq. 7 can be modified as:

$$V_j = C'_s + C'_c + N_b/2 - V_2 \quad (8)$$

In Eq. 8, the beam axial load N_b can be evaluated using the proposed equation, Eq. 6.

To avoid the formation of plastic hinge in columns, many codes suggests that the flexural

strength ratio at joint, defined as the ratio between the sum of the moments of the columns, $\sum M_c$, to the sum of the moments of beams, $\sum M_b$, framing into the joint, should be larger than unity. As an example the ACI code [10] suggests that the ratio should be larger than 1.20. For LN60 frame, the generated axial force at mid-span of the beam, reduced the flexural strength ratio at joint of about 14%. This amount of reduction is very important and can lead to the formation of plastic hinge in columns before beams.

5. CONCLUSIONS

Experimental and analytical results of two 1/2-scale RC frames were reported in this paper. The main conclusions of this research program are summarized as follows:

1. Axial load in beams are generally neglected during the design process. However, from the experiment an axial load of 33% of the frame horizontal load carrying capacity was generated at the first story beam.
2. The envelope curves of the load-drift relationship for the frames were predicted with a good accuracy using a pushover analysis with the plastic hinge characteristics for beams and columns as suggested by the Japanese design guidelines.
3. It is suggested that double curvature column should be tested instead of single curvature column test, cantilever column, in order to take into account the shift of the Contraflexure point.
4. The joint shear force and the flexural strength ratio at a joint have to be assessed by taking into account the probable axial loads that can be generated in beams. The beam axial load is due to the beam elongation as a consequence of the damage that occurs at the beam plastic hinge regions.

More tests are needed to investigate the effect of slabs on the beam elongation and on the axial load intensity.

ACKNOWLEDGEMENT

The authors thanks Mr. Koji Shinomiya and Yoko Yasutomi former student at Kyoto University. The first author is thankful to the JSPS's financial support.

REFERENCES

- [1] Bechtoula, H., Arai, Y., Kono, S., Watanabe,

- F., "Damage Assessment of RC Columns Under Large Axial and Lateral Loadings," Symposium on a design procedure of RC structures based on inelastic deformation -Use of confined concrete-, pp. 263-270, November 30, 2001
- [2] Fenwick, R. C. and Megget, L.M., "Elongation and load deflection characteristics of reinforced concrete members containing plastic hinges," Bulletin on the National Society for Earthquake Engineering, 26(1), pp. 28-41, 1993.
- [3] Kono, S., Bechtoula, H., Sakashita, M., Watanabe, F., Tanaka, H., Nishiyama, M. and Eberhard, M. O., "Damage evaluation of RC columns under multiaxial loadings," US-Japan cooperation research on urban earthquake disaster mitigation, Kyoto Japan, pp. 157-193, March 2004.
- [4] John F. Stanton and Suzanne D. Nakaki, "Design guidelines for precast concrete seismic structural systems," PRESS Report No. 01/03-09, UW Report No. SM 02-02, January 2002.
- [5] Jubum Kim, "Behavior of hybrid frames under seismic loading," Dissertation submitted in partial fulfillment of the requirement for the degree of the Doctor of Philosophy, University of Washington, 2002.
- [6] Bechtoula Hakim, "Seismic Performance of Moderate or Low Rise Reinforced Concrete Frame Building," Dissertation submitted in partial fulfillment of the requirement for the degree of the Doctor of Engineering, Kyoto University, 2005.
- [7] SAP2000, linear and nonlinear static and dynamic analysis and design of three-dimensional structures, Integrated Finite Elements Analysis and Design of Structures, a product of Computer & structures, Inc., Version 8.0, June 2002.
- [8] Architecture Institute of Japan AIJ, Design guidelines for earthquake resistant reinforced concrete buildings based on inelastic concept 1999.
- [9] Hanson, Norman W. and Harold W. Connor, "Seismic Resistance of Reinforced Concrete Beam-Column Joint," Journal of the Structural Division, Vol. 93, ST5, pp.533-560, Oct.1967.
- [10] American Concrete Institute, Building Code Requirements for Structural Concrete (ACI 318-02) and Commentary (ACI 318R-02).